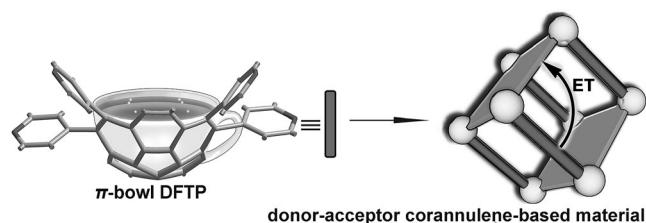# Hierarchical Corannulene-Based Materials: Energy Transfer and Solid-State Photophysics

Allison M. Rice, W. Brett Fellows, Ekaterina A. Dolgopolova, Andrew B. Greytak, Aaron K. Vannucci, Mark D. Smith, Stavros G. Karakalos, Jeanette A. Krause, Stanislav M. Avdoshenko,* Alexey A. Popov, and Natalia B. Shustova*

Abstract: We report the first example of a donor–acceptor corannulene-containing hybrid material with rapid ligand-to-ligand energy transfer (ET). Additionally, we provide the first time-resolved photoluminescence (PL) data for any corannulene-based compounds in the solid state. Comprehensive analysis of PL data in combination with theoretical calculations of donor–acceptor exciton coupling was employed to estimate ET rate and efficiency in the prepared material. The ligand-to-ligand ET rate calculated using two models is comparable with that observed in fullerene-containing materials, which are generally considered for molecular electronics development. Thus, the presented studies not only demonstrate the possibility of merging the intrinsic properties of π-bowls, specifically corannulene derivatives, with the versatility of crystalline hybrid scaffolds, but could also foreshadow the engineering of a novel class of hierarchical corannulene-based hybrid materials for optoelectronic devices.

Scheme 1. A schematic of the hybrid donor–acceptor corannulene-based material with rapid energy transfer prepared from the corannulene-based linker. A grey rod represents the donor while the grey plate is an acceptor.

While the compromise between strain and aromaticity is a persistent synthetic challenge,[1–3] the bowl shape and electronic properties of corannulene derivatives (buckybowls, Scheme 1) imply an unrevealed potential for molecular electronics development similar to their close famous analogues, fullerenes. The main success of the latter in the field of optoelectronics is associated with very fast energy/electron transfer, which has been demonstrated in numerous photo-physical studies.[4–6] In contrast, development of buckybowl-containing materials with desirable properties is still in its infancy. For instance, during the 50 years since the discovery of the first solution route for corannulene preparation (1966),[1] only around 20 papers[2,7–32] include any photo-physical studies, despite nearly 1000 publications focused on corannulene. To the best of our knowledge, there are only two reports[8,10] in the area of corannulene solid-state photophysics. Furthermore, no solid-state time-resolved photo-luminescence (PL) data or energy transfer (ET) studies have been reported for any corannulene-containing compounds despite the fact that ET rate and efficiency are crucial fundamental parameters for applications ranging from organic photovoltaics to photocatalysis.[33,34] This gap in material development was the major driving force to initiate the presented study, especially taking into account the recent progress in corannulene chemistry.[35]

Our shift from more traditional flat aromatic hydrocarbons[36] towards π-bowls (for example, corannulene) was also driven by 1) their significant dipole moment, 2) the possibility to extend the dimensionality of 3D hybrid frameworks through the π-bowl curvature, 3) potential for charge stabilization on the surface owing to doubly degenerate lowest unoccupied molecular orbitals (LUMOs), 4) anticipated effective intermolecular charge transport, and 5) presence of theoretically predicted super atomic molecular orbitals, which are key factors for intermolecular charge/energy transport distinct from the conventional mechanisms involving π molecular orbital overlap.[37–41] The latter two facts were among the main reasons that influenced the choice of the π-bowl, in particular corannulene, in our studies.

Herein, we report the first example of a donor–acceptor (D–A) corannulene-based material with rapid ligand-to-ligand ET, similar to that observed in fullerene-containing compounds.[4] The reported hybrid is also the first crystalline

[*] A. M. Rice, Dr. W. B. Fellows, E. A. Dolgopolova,
Prof. Dr. A. B. Greytak, Prof. Dr. A. K. Vannucci, Dr. M. D. Smith,
Prof. Dr. N. B. Shustova
Department of Chemistry and Biochemistry, University of South Carolina
631 Sumter Street, Columbia, SC 29208 (USA)
E-mail: shustova@sc.edu

Dr. S. G. Karakalos
College of Engineering and Computing, Swearingen Engineering Center
Columbia, SC 29208 (USA)

Dr. J. A. Krause
Department of Chemistry, University of Cincinnati
Cincinnati, OH 45221 (USA)

Dr. S. M. Avdoshenko, Dr. A. A. Popov
Leibniz Institute for Solid State and Materials Research
01069 Dresden (Germany)
E-mail: s.avdoshenko@gmail.com

Supporting information, including full experimental details, photo-luminescence data, and theoretical calculations, and the ORCID identification number(s) for the author(s) of this article can be found under:
http://dx.doi.org/10.1002/anie.201612199.

buckybowl-containing extended structure, in which control over corannulene (donor)–acceptor orientation is achieved through covalent bonding (Scheme 1). A synthetic route to the novel multidentate building block, which provides the necessary versatility for preparation of crystalline corannulene-based multidimensional materials, has also been established. To achieve the required D–A spectral overlap and study ET processes, we utilized the advantages offered by well-defined hybrids including modularity and tunability.[33,34] Based on time-resolved PL data and theoretical studies of D–A exciton coupling, the ET efficiency and rate, key factors for application development in the field of optoelectronics,[42–49] were estimated. Thus, the presented studies provide an opportunity to shed light on ET processes in corannulene-based material for the first time.

The initial challenge in the preparation of the aforementioned donor–acceptor corannulene materials mainly lies in synthesis of the versatile corannulene-containing building blocks on gram or larger scales. Therefore, scalability and reaction yield were two initial factors considered for preparation of a novel 4,4′,4″,4‴-(dibenzo[ghi,mno]fluoranthene-1,2,5,6-tetrayl)tetrapyridine linker (DFTP, Figure 1 and the Supporting Information, Figure S1 and Scheme S1).

Figure 1 demonstrates DFTP molecular packing, which consists of layers containing offset "clamshells", in contrast to many corannulene derivatives exhibiting convex–concave stacking (Supporting Information, Figure S2).[50–52] Further synthetic and characterization details, including cyclic voltammetry of DFTP, can be found in the Supporting Information (Figures S3–S6 and Table S2). Since no solid-state time-resolved data are available for any corannulene-based materials (including parent corannulene ($C_{20}H_{10}$)), we have studied the photophysical response of DFTP by steady-state

and time-resolved photoluminescence spectroscopy, and, therefore, established a reference point for material characterization. The amplitude-weighted average solid-state lifetime was found to be 5.9 ns for DFTP, which is shorter compared to the measured values for $C_{20}H_{10}$ itself (9.1 ns) or tetrakis(4-carboxyphenyl)corannulene[8] (9.6 ns, the instrument response function and PL decays are shown in the Supporting Information, Figure S7).

To test the possibility of DFTP to form extended structures and, therefore, gain structural insights into viable topologies, as well as probe the photophysical properties of DFTP-based materials, we studied the coordination of DFTP to metal ions. The metal was mainly chosen to prevent material photoluminescence quenching (for example, d^0 and d^{10} metals). The synthesized two-dimensional (2D) framework $[Ag_2(DFTP)_2](PF_6)_2 \cdot (C_6H_6)_6 \cdot (CH_3CN)_3$ (**1**) was characterized by single-crystal and powder X-ray diffraction (PXRD), thermogravimetric analysis, and Fourier transform infrared (FT-IR) spectroscopy (Figure 1 and the Supporting Information, Figures S8–S10 and Table S3). The single-crystal X-ray studies revealed preservation of the DFTP curvature inside **1**, despite the possibility to flatten or lock the molecular confirmation with high strain energy imposed by framework rigidity.[53] Indeed, the bowl depth of DFTP inside **1** (0.85 Å, Figure 1) is essentially that of parent corannulene (0.87 Å[54]). Owing to the curvature preservation, the DFTP bowl could fit solvent molecules such as benzene (Figure 1). Thus, the curvature of corannulene-based linkers could pave the way for an extension of framework dimensionality beyond changing the metal node geometry and linker length.

The studies of the photophysical properties of **1** showed ligand-centered luminescence (Figure 2 a). The emission maximum of **1** was observed at 503 nm ($\lambda_{ex} = 350$ nm), similar to that for the free ligand (see above). Analysis of the curves with a reconvolution fit supported a triexponential decay
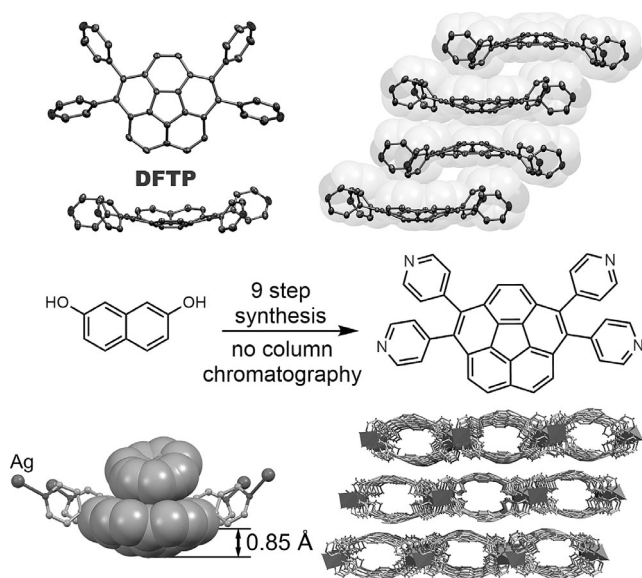

Figure 1. (top) The single-crystal X-ray structure and offset "clamshell" crystal packing of DFTP. Displacement ellipsoids are drawn at the 60% probability level.[60] (middle) A synthetic scheme for the DFTP linker. (bottom) Packing of **1** and a part of **1** showing the bowl depth of DFTP. Space-filling models show the fit of the solvent molecule (benzene) inside **1**.
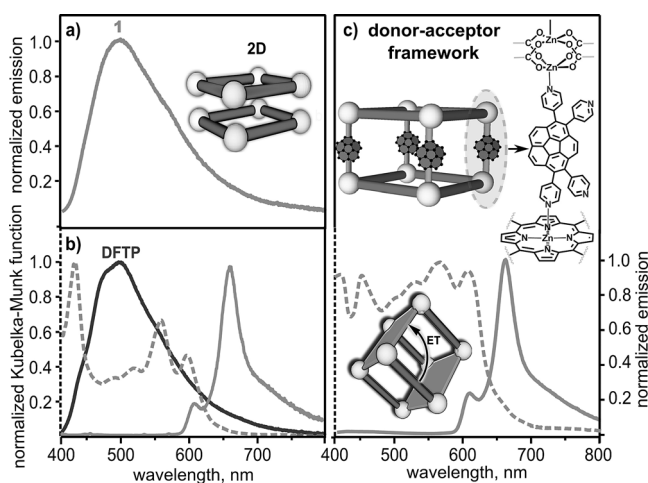

Figure 2. a) The normalized emission spectrum of **1**. b) Normalized diffuse reflectance (•••••) and emission (——) spectra of the porphyrin-based framework (acceptor). The normalized emission spectrum of DFTP (donor, ——). c) A schematic of donor–acceptor **2**. The normalized diffuse reflectance (•••••) and emission (——) spectra of **2**. An excitation wavelength of 350 nm was used to acquire all photoluminescence spectra.

model, for which the amplitude-weighted average lifetime of **1** was found to be 3.4 ns (Figure S7). This lifetime is slightly shorter in comparison with that (4.1 ns) of another example of a corannulene-based framework, $[Cd_2(C_{48}H_{22}O_8)(DMA)_3]\cdot$ $(DMA)_{1.7}$, (DMA = dimethylacetamide) consisting of tetrakis(4-carboxyphenyl)corannulene linker (see the Supporting Information for Cd-based framework synthesis and characterization, Figures S11 and S12, and Table S3).

As the next step, we applied our findings to the preparation of a crystalline D–A framework, in which the mutual orientation of the donor (D) and acceptor (A) was controlled through covalent bond formation. In general, for synthesis of D–A materials possessing resonance ET, the emission spectrum of D should overlap with the absorption profile of A.[33,55] In our case, to design a material in which the corannulene-based linker, DFTP, could serve as D, we selected 2D $Zn_2(ZnTCPP)$[56] (H_4TCPP = tetrakis(4-carboxyphenyl) porphyrin) as A. Figure 2b shows the diffuse reflectance profile of A, which absorbs light up to 650 nm, and therefore provides the necessary spectral overlap of its absorption profile with the emission response of DFTP (D).[55]

For rational D–A organization, we utilized a two-step synthetic route, which relies on preparation of the Zn_2-(ZnTCPP) scaffold, followed by coordinative immobilization of DFTP (D) as a pillar between the layers (Figure 2c and the Supporting Information, Figure S13). In addition to the photophysical requirements, the presence of metal sites, which serve as anchors for coordination of the pyridyl groups, was an additional criterion for framework selection. The coordinative immobilization of DFTP between the Zn_2(ZnTCPP) layers was achieved by coordination of the pyridyl groups of the linker to the metal in the $Zn_2(O_2C^-)_4$ nodes (Figure 2c and the Supporting Information, Figure S14) and resulted in formation of $[Zn_2(ZnTCPP)-(DFTP)_{0.69}(DMF)_{0.31}]\cdot(DMF)_{0.3}\cdot(H_2O)_{26}$ (**2**). The diffuse reflectance and emission profiles of **2** are shown in Figure 2c. The latter shows that the incorporation of both donor and acceptor moieties in **2** resulted in the almost complete disappearance of donor emission (Figure 2c), which could be attributed to efficient ET. A comprehensive analysis of the prepared D–A material **2** was performed by PXRD, elemental analysis, FT-IR spectroscopy, epifluorescence microscopy, X-ray photoelectron spectroscopy, theoretical modeling, NMR spectroscopy, and mass spectrometry (the latter two techniques were performed on digested samples of **2**, Figures S14–S21; more details about characterization of **2** can be found in the Supporting Information).

To quantitatively describe the possibility of resonance ET, time-resolved photoluminescence spectroscopy was employed. In particular, analysis of time-resolved PL decays was performed for D (DFTP) in the absence and presence of A (Zn_2(ZnTCPP)). The emission wavelength channel was configured to capture the DFTP emission and exclude the PL response of the porphyrin-based acceptors. Figure 3 shows that the time-resolved photoluminescence curve for coordinatively immobilized DFTP in the presence of the porphyrin-containing acceptor decays more rapidly than that of non-coordinated DFTP. Analysis of the curves with a reconvolu-
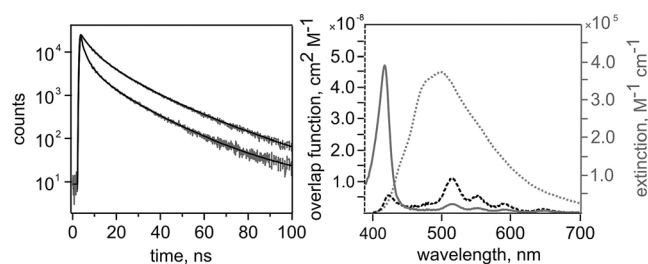

Figure 3. (left) Fluorescence decays of DFTP in the solid state (top) and coordinatively immobilized inside the crystalline donor–acceptor corannulene-based scaffold (bottom). (right) Förster analysis of **2** illustrating the spectral overlap function (-----, left vertical axis) calculated for the measured emission spectrum of DFTP (dotted grey line, arbitrary scale) and the molar extinction spectrum of H_4TCPP in ethanol (solid grey line, right vertical axis).

tion fit supported a triexponential decay model, which revealed an 85% reduction of the amplitude-weighted average lifetime, from 5.9 ns (DFTP) to 0.85 ns (**2**).

As the first approximation to estimate ET rate (k_{ET}) and efficiency, we applied the classical Förster resonance ET approach [Eq. (S3), see the Supporting Information],[55] in which the corresponding ET efficiency and k_{ET} in **2** were found to be 85% and 1.01×10^9 s^{-1}, respectively. Notably, the observed ligand-to-ligand ET efficiency is approximately 1.7-fold higher than that reported for a recent fullerene-based hybrid material, in which the fullerene-based linker serves as an acceptor.[57] To address the possibility of resonance ET within this model, we estimated the Förster critical transfer radius, R_o, for randomly-oriented point dipoles with the same spectral overlap, J, as the DFTP (D) and 2D porphyrin-based A, which was $J = 8.3 \times 10^{-14}$ cm^3 M^{-1} [Eq. (S4), Figure 3].[55] The resulting R_o value of approximately 31 Å [Eq. (S5)] is far beyond the D–A distance approximated from the structural data. Therefore, we could attribute the observed changes in the D profile after coordinative immobilization to resonance ET.

To apply a more generalized approach, which would allow estimation of k_{ET} beyond the point-dipole model described above, we have also calculated k_{ET} based on $k_{ET} = 2\pi V^2 J_e/\hbar$[58] [where V = D–A exciton coupling and J_e = spectral overlap function,[58] calculated from Eq. (S6)]. While J_e was estimated from the experimental data [Eq. (S6)], V was obtained from ab initio calculations based on structural data for **2** [Eq. (S11)]. Previous theoretical studies for a similar class of hybrid systems demonstrated that frontier orbitals have a localized nature near the Fermi level.[57] Similarly, the periodic hybrid material **2** will have no dispersion of relevant bands. Therefore, a truncated model, instead of the complete 3D periodic D–A framework, was utilized for theoretical studies. For estimation of V, we employed recent theoretical models focusing on strong orbital coupling, since in our case, D and A are covalently bonded (the model description and specific equations can be found in the Supporting Information). Figure 4 shows an excited state diagram complemented by molecular orbitals contributing to the excitations. The first four excited states of the truncated model of **2** are represented by two-fold degenerated excitations (Q-type and Soret bands) in the $H_4ZnTCPP$ fragment, with energies of approximately
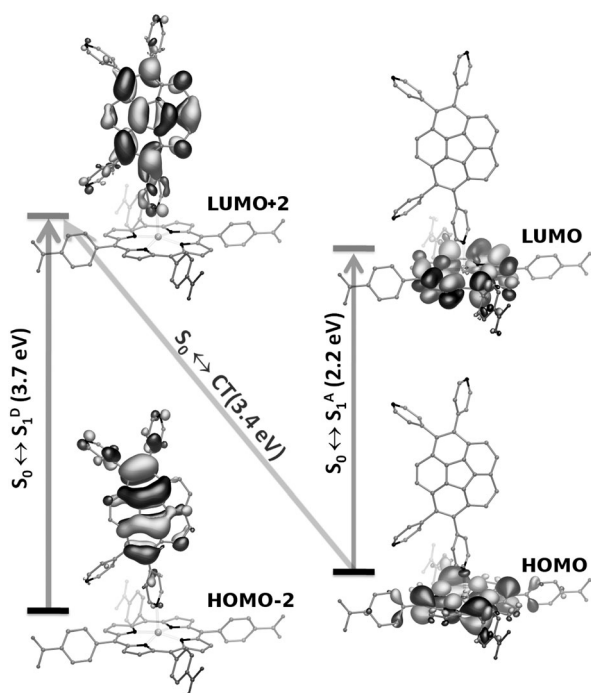
Figure 4. A schematic of the excitation diagram and most prominent molecular orbitals of each excitation.

2.2 eV and 3.3 eV, respectively. The excited state that dominated the excitation of DFTP has an energy of 3.7 eV ($\lambda_{ex} = 3.54$ eV). Therefore, there are two possible ET mechanisms in the considered model. The first mechanism involves a direct coupling between S_1^D and S_1^A/S_2^A states. The alternative route includes the formation of a charge transfer (CT) complex, with a CT excitation energy of 3.4 eV. In the latter case, the excitation will still be localized on the DFTP fragment, which could result in PL quenching, assuming large exciton coupling between CT and S_1^A/S_2^A states. According to our calculations, the $S_1^D \leftrightarrow S_1^A$ excitations have a large coupling $V = 200$ meV [Eq. (S11)], while estimated coupling in the case of other possibilities ($S_1^D \leftrightarrow S_2^A$, $CT \leftrightarrow S_1^A$, $CT \leftrightarrow S_2^A$) is much smaller (ca. 1 meV). Moreover, the CT excitation molecular orbitals (HOMO and LUMO−2) are arranged almost orthogonally, which suggests a small probability of electron transfer. Based on those considerations, we may conclude that the ET process, $S_1^D \leftrightarrow S_1^A$, is likely to be a dominating relaxation mechanism in the D–A system. Taking into account the estimated values of exciton coupling, V, and spectral overlap function, J_e [1.2×10^{-4} eV^{-1}, Eq. (S6)], we found k_{ET} to be 4.5×10^{10} s^{-1}. Thus, both models for k_{ET} predict rapid ET in the prepared D–A system. In spite of the donating role of DFTP in the presented studies, consideration of corannulene as the smallest bowl-shaped fullerene fragment provoked us to analyze the ET rates previously reported for D–A fullerene-based scaffolds. For instance, k_{ET} in an example with a porphyrin (D)–fullerene (A) system was 5.0×10^9 s^{-1},[59] which is comparable with the rate observed in our corannulene–porphyrin-based D–A framework.

The foregoing results demonstrate the first example of a D–A corannulene-based material **2** with rapid ligand-to-ligand ET. Preparation of **2** was possible due to the synthesis

of the novel multidentate building block, DFTP, suitable for the preparation of multidimensional corannulene-based materials such as **1** and **2**, available on a gram-scale due to recent achievements in corannulene chemistry. The presented study is also the first report of solid-stale time-resolved PL data collected for any corannulene-containing compound, including parent $C_{20}H_{10}$. Comprehensive analysis of PL decays in combination with theoretical studies of spectral overlap function and D–A exciton coupling revealed that the ligand-to-ligand ET rate estimated from two models is comparable with that observed in fullerene-containing materials, which are generally considered as building blocks for molecular electronics development. In addition, the ligand-to-ligand ET efficiency of **2** is 1.7-fold higher than that estimated for the fullerene–porphyrin hybrid material.[57]

To summarize, by using theoretical modeling in combination with spectroscopic studies, we shed light on solid-state photophysics (including the possible mechanisms of energy transfer) of a D–A corannulene-containing framework, which is crucial fundamental knowledge required for the successful implementation of any corannulene derivative in a wide number applications ranging from solar cells to photocatalysts, as well as sensors and photoswitches. Thus, the presented study not only demonstrates the possibility of merging the intrinsic properties of π-bowls with the versatility of metal–organic frameworks but could also foreshadow the engineering of a novel class of corannulene-based hybrid materials for optoelectronic devices.

Conflict of interest

The authors declare no conflict of interest.

[1] W. E. Barth, R. G. Lawton, *J. Am. Chem. Soc.* **1966**, *88*, 380–381.
[2] A. S. Filatov, A. V. Zabula, S. N. Spisak, A. Y. Rogachev, M. A. Petrukhina, *Angew. Chem. Int. Ed.* **2014**, *53*, 140–145; *Angew. Chem.* **2014**, *126*, 144–149.

4   www.angewandte.org

▶▶ These are not the final page numbers!

© 2017 Wiley-VCH Verlag GmbH & Co. KGaA, Weinheim

Angew. Chem. Int. Ed. **2017**, *56*, 1–6

[3] S. Lampart, L. M. Roch, A. K. Dutta, Y. Wang, R. Warshaman-age, A. D. Finke, A. Linden, K. K. Baldridge, J. S. Siegel, *Angew. Chem. Int. Ed.* **2016**, *55*, 14648–14652; *Angew. Chem.* **2016**, *128*, 14868–14872.

[4] J. Sukegawa, C. Schubert, X. Zhu, H. Tsuji, D. M. Guldi, E. Nakamura, *Nat. Chem.* **2014**, *6*, 899–905.

[5] K. P. Castro, Y. Jin, J. J. Rack, S. H. Strauss, O. V. Boltalina, A. A. Popov, *J. Phys. Chem. Lett.* **2013**, *4*, 2500–2507.

[6] C.-Z. Li, H.-L. Yip, A. K.-Y. Jen, *J. Mater. Chem.* **2012**, *22*, 4161–4177.

[7] P. Liu, Y. Hisamune, M. D. Peeks, B. Odell, J. Q. Gong, L. M. Herz, H. L. Anderson, *Angew. Chem. Int. Ed.* **2016**, *55*, 8358–8362; *Angew. Chem.* **2016**, *128*, 8498–8502.

[8] W. B. Fellows, A. M. Rice, D. E. Williams, E. A. Dolgopolova, A. K. Vannucci, P. J. Pellechia, M. D. Smith, J. A. Krause, N. B. Shustova, *Angew. Chem. Int. Ed.* **2016**, *55*, 2195–2199; *Angew. Chem.* **2016**, *128*, 2235–2239.

[9] M. Yamada, K. Ohkubo, M. Shionoya, S. Fukuzumi, *J. Am. Chem. Soc.* **2014**, *136*, 13240–13248.

[10] A. S. Filatov, E. A. Jackson, L. T. Scott, M. A. Petrukhina, *Angew. Chem. Int. Ed.* **2009**, *48*, 8473–8476; *Angew. Chem.* **2009**, *121*, 8625–8628.

[11] J. Dey, A. Y. Will, R. A. Agbaria, P. W. Rabideau, A. H. Abdourazak, R. Sygula, I. M. Warner, *J. Fluoresc.* **1997**, *7*, 231–236.

[12] M. Yamaji, K. Takehira, T. Mikoshiba, S. Tojo, Y. Okada, M. Fujitsuka, T. Majima, S. Tobita, J. Nishimura, *Chem. Phys. Lett.* **2006**, *425*, 53–57.

[13] Y.-T. Wu, D. Bandera, R. Maag, A. Linden, K. K. Baldridge, J. S. Siegel, *J. Am. Chem. Soc.* **2008**, *130*, 10729–10739.

[14] Y. Kim, M. Lee, *Chem. Eur. J.* **2015**, *21*, 5736–5740.

[15] A. K. Dutta, A. Linden, L. Zoppi, K. K. Baldridge, J. S. Siegel, *Angew. Chem. Int. Ed.* **2015**, *54*, 10792–10796; *Angew. Chem.* **2015**, *127*, 10942–10946.

[16] G. Valenti, C. Bruno, S. Rapino, A. Fiorani, E. A. Jackson, L. T. Scott, F. Paolucci, M. Marcaccio, *J. Phys. Chem. C* **2010**, *114*, 19467–19472.

[17] J. Mack, P. Vogel, D. Jones, N. Kaval, A. Sutton, *Org. Biomol. Chem.* **2007**, *5*, 2448–2452.

[18] G. H. Grube, E. L. Elliott, R. J. Steffens, C. S. Jones, K. K. Baldridge, J. S. Siegel, *Org. Lett.* **2003**, *5*, 713–716.

[19] T. J. Seiders, E. L. Elliott, G. H. Grube, J. S. Siegel, *J. Am. Chem. Soc.* **1999**, *121*, 7804–7813.

[20] D. Wu, T. Shao, J. Men, X. Chen, G. Gao, *Dalton Trans.* **2014**, *43*, 1753–1761.

[21] Y.-L. Wu, M. C. Stuparu, C. Boudon, J.-P. Gisselbrecht, W. B. Schweizer, K. K. Baldridge, J. S. Siegel, F. Diederich, *J. Org. Chem.* **2012**, *77*, 11014–11026.

[22] N. Niamnont, N. Kimpitak, K. Wongravee, P. Rashatasakhon, K. K. Baldridge, J. S. Siegel, M. Sukwattanasinitt, *Chem. Commun.* **2013**, *49*, 780–782.

[23] Y. Matsuo, K. Tahara, M. Sawamura, E. Nakamura, *J. Am. Chem. Soc.* **2004**, *126*, 8725–8734.

[24] M. C. Stuparu, *Tetrahedron* **2012**, *68*, 3527–3531.

[25] F. Hauke, S. Atalick, D. M. Guldi, J. Mack, L. T. Scott, A. Hirsch, *Chem. Commun.* **2004**, 766–767.

[26] S. Ito, Y. Tokimaru, K. Nozaki, *Angew. Chem. Int. Ed.* **2015**, *54*, 7256–7260; *Angew. Chem.* **2015**, *127*, 7364–7368.

[27] Y. Matsuo, Y. Sato, M. Hashiguchi, K. Matsuo, E. Nakamura, *Adv. Funct. Mater.* **2009**, *19*, 2224–2229.

[28] C. S. Jones, E. Elliott, J. S. Siegel, *Synlett* **2004**, 187–191.

[29] M. Mattarella, L. Berstis, K. K. Baldridge, J. S. Siegel, *Bioconjugate Chem.* **2014**, *25*, 115–128.

[30] Y. Wang, Y. Li, W. Zhu, J. Liu, X. Zhang, R. Li, Y. Zhen, H. Dong, W. Hu, *Nanoscale* **2016**, *8*, 14920–14924.

[31] H. Barbero, S. Ferrero, L. Alvarez-Miguel, P. Gomez Iglesias, D. Miguel, C. M. Alvarez, *Chem. Commun.* **2016**, *52*, 12964–12967.

[32] R. Chen, R.-Q. Lu, P.-C. Shi, X.-Y. Cao, *Chin. Chem. Lett.* **2016**, *27*, 1175–1183.

[33] D. E. Williams, N. B. Shustova, *Chem. Eur. J.* **2015**, *21*, 15474–15479.

[34] T. Zhang, W. Lin, *Chem. Soc. Rev.* **2014**, *43*, 5982–5993.

[35] A. M. Butterfield, B. Gilomen, J. S. Siegel, *Org. Process Res. Dev.* **2012**, *16*, 664–676.

[36] H. Oshima, A. Fukazawa, S. Yamaguchi, *Angew. Chem. Int. Ed.* **2017**, *56*, 3270–3274; *Angew. Chem.* **2017**, *129*, 3318–3322.

[37] A. V. Zabula, A. Y. Rogachev, M. A. Petrukhina, *Science* **2011**, *333*, 1008–1011.

[38] A. Ayalon, A. Sygula, P. C. Cheng, M. Rabinovitz, P. W. Rabideau, L. T. Scott, *Science* **1994**, *265*, 1065–1067.

[39] L. Zoppi, L. Martin-Samos, K. K. Baldridge, *Phys. Chem. Chem. Phys.* **2015**, *17*, 6114–6121.

[40] L. M. Roch, L. Zoppi, J. S. Siegel, K. K. Baldridge, *J. Phys. Chem. C* **2017**, *121*, 1220–1234.

[41] L. Zoppi, J. S. Siegel, K. K. Baldridge, *Wiley Interdiscip. Rev.: Comput. Mol. Sci.* **2012**, *3*, 1–12.

[42] L. E. Kreno, K. Leong, O. K. Farha, M. Allendorf, R. P. Van Duyne, J. T. Hupp, *Chem. Rev.* **2012**, *112*, 1105–1125.

[43] Z. Guo, D. K. Panda, K. Maity, D. Lindsey, T. G. Parker, T. E. Albrecht-Schmitt, J. L. Barreda-Esparza, P. Xiong, W. Zhou, S. Saha, *J. Mater. Chem. C* **2016**, *4*, 894–899.

[44] H. Furukawa, K. E. Cordova, M. O'Keeffe, O. M. Yaghi, *Science* **2013**, *341*, 1230444.

[45] B. Manna, S. Singh, A. Karmakar, A. V. Desai, S. K. Ghosh, *Inorg. Chem.* **2015**, *54*, 110–116.

[46] K. Sasan, Q. Lin, C. Mao, P. Feng, *Nanoscale* **2016**, *8*, 10913–10916.

[47] W. P. Lustig, F. Wang, S. J. Teat, Z. Hu, Q. Gong, J. Li, *Inorg. Chem.* **2016**, *55*, 7250–7256.

[48] F. Wang, W. Liu, S. J. Teat, F. Xu, H. Wang, X. Wang, L. An, J. Li, *Chem. Commun.* **2016**, *52*, 10249–10252.

[49] D. F. Sava, L. E. S. Rohwer, M. A. Rodriguez, T. M. Nenoff, *J. Am. Chem. Soc.* **2012**, *134*, 3983–3986.

[50] B. Topolinski, B. M. Schmidt, S. Schwagerus, M. Kathan, D. Lentz, *Eur. J. Inorg. Chem.* **2014**, 5391–5405.

[51] C. Dubceac, A. S. Filatov, A. V. Zabula, M. A. Petrukhina, *Cryst. Growth Des.* **2015**, *15*, 778–785.

[52] I. V. Kuvychko, S. N. Spisak, Y.-S. Chen, A. A. Popov, M. A. Petrukhina, S. H. Strauss, O. V. Boltalina, *Angew. Chem. Int. Ed.* **2012**, *51*, 4939–4492; *Angew. Chem.* **2012**, *124*, 5023–5026.

[53] N. B. Shustova, A. F. Cozzolino, M. Dincă, *J. Am. Chem. Soc.* **2012**, *134*, 19596–19599.

[54] J. C. Hanson, C. E. Nordman, *Acta Crystallogr.* **1976**, *32*, 1147–1153.

[55] J. R. Lakowicz, *Principles of Fluorescence Spectroscopy*, Springer, **2007**.

[56] B. J. Burnett, W. Choe, *CrystEngComm* **2012**, *14*, 6129–6131.

[57] D. E. Williams, E. A. Dolgopolova, D. C. Godfrey, E. D. Ermolaeva, P. J. Pellechia, A. B. Greytak, M. D. Smith, S. M. Avdoshenko, A. A. Popov, N. B. Shustova, *Angew. Chem. Int. Ed.* **2016**, *55*, 9070–9074; *Angew. Chem.* **2016**, *128*, 9216–9220.

[58] Q. Zhang, C. Zhang, L. Cao, Z. Wang, B. An, Z. Lin, R. Huang, Z. Zhang, C. Wang, W. Lin, *J. Am. Chem. Soc.* **2016**, *138*, 5308–5315.

[59] Y. Kuramochi, A. Satake, A. S. D. Sandanayaka, Y. Araki, O. Ito, Y. Kobuke, *Inorg. Chem.* **2011**, *50*, 10249–10258.

[60] CCDC 1519743 (DFTP), 1519908 (**1**), and 1519742 (Cd-framework) contain the supplementary crystallographic data for this paper. These data are provided free of charge by The Cambridge Crystallographic Data Centre.
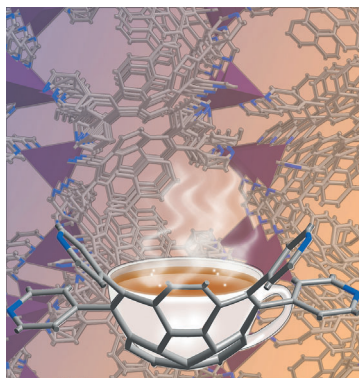
Communications

Supramolecular Chemistry

A. M. Rice, W. B. Fellows,
E. A. Dolgopolova, A. B. Greytak,
A. K. Vannucci, M. D. Smith,
S. G. Karakalos, J. A. Krause,
S. M. Avdoshenko,* A. A. Popov,
N. B. Shustova* —————— ▮▮▮▮–▮▮▮▮

Hierarchical Corannulene-Based
Materials: Energy Transfer and Solid-
State Photophysics

But first, coffee: A rapid ligand-to-ligand energy transfer observed in the first example of a donor–acceptor corannulene-based scaffold is similar to the energy that a cup of coffee could provide. Many components can be added to the corannulene bowl, similar to cream and sugar added to coffee, highlighting the possibility of merging the intrinsic properties of π-bowls with the tunability of hierarchical materials for applications in optoelectronic devices.

6   www.angewandte.org

↖↖ These are not the final page numbers!

© 2017 Wiley-VCH Verlag GmbH & Co. KGaA, Weinheim

Angew. Chem. Int. Ed. **2017**, *56*, 1–6